# Generalized Frequency Division Multiplexing with Space and Frequency Index Modulation

Ersin Öztürk[1,2], Ertugrul Basar[1], Hakan Ali Çırpan[1]
[1]Istanbul Technical University, Faculty of Electrical and Electronics Engineering, 34469, Maslak, Istanbul, Turkey
Email: {ersinozturk, basarer, cirpanh}@itu.edu.tr
[2]Netas, Department of Research and Development, 34912, Pendik, Istanbul, Turkey
Email: eozturk@netas.com.tr

***Abstract*—Generalized frequency division multiplexing (GFDM) has been regarded as one of the promising candidates for the physical layer (PHY) of fifth generation (5G) wireless networks. Multiple-input multiple-output (MIMO) friendliness is a key ability for a physical layer scheme to match the foreseen requirements of 5G wireless networks. On the other hand, index modulation (IM) concept, which relies on conveying additional information bits through indices of certain transmit entities, is an emerging technique to provide better spectral efficiency. In this paper, a novel MIMO-GFDM system, which combines GFDM with space and frequency IM (SFIM) technique, is proposed. In the GFDM-SFIM scheme, the transmit antenna, the constellation mode and the classic constellation symbols are determined according to incoming bit stream. The main contribution of the paper is the construction of the GFDM-SFIM system model including joint MIMO detection and GFDM demodulation performed by the GFDM-SFIM receiver. We evaluate the error performance of the GFDM-SFIM scheme as well as prove its superiority by making comparisons with the spatial modulation (SM) GFDM system and orthogonal frequency division multiplexing (OFDM) SFIM system for Rayleigh multipath fading channels.**

## I. Introduction

Generalized frequency division multiplexing (GFDM) has been proposed as one of the candidates for the air interface of fifth generation (5G) wireless networks [1]. Flexible time-frequency partitioning through $K$ subcarriers with $M$ timeslots, reduced out-of-band (OOB) emission by circular pulse shaping and improved spectral efficiency due to single cyclic prefix (CP) usage for entire symbol block make GFDM a promising physical layer (PHY) solution among many proposed waveforms.

The continuing demand for higher data rates motivates the researchers to seek spectrum-efficient modulation schemes. Spatial modulation (SM) is a multiple-input multiple-output (MIMO) transmission method, which considers the transmit antennas as spatial constellation points to carry additional information bits [2]. Orthogonal frequency division multiplexing (OFDM) with index modulation (IM) is an extension of the SM concept to subcarrier indices in multicarrier systems [3]–[5]. In OFDM-IM, active subcarriers are selected by the input bit sequences and the information bits are conveyed by both the activated subcarrier indices and the conventional modulation symbols. In [6], a dual-mode OFDM-IM (DM-OFDM) scheme has been proposed to prevent throughput loss in OFDM-IM due to unused subcarriers. In the DM-OFDM scheme, based on the OFDM subcarrier group concept in [3], two different constellation modes have been used to modulate the selected subcarrier indices and the remaining subcarriers in a subcarrier group. Furthermore, in [7] and [8], combination of IM technique with MIMO methods, namely space and frequency IM (SFIM), has been investigated and significant performance gains have been reported.

MIMO-friendliness is a key ability for a PHY scheme to match the foreseen requirements of 5G wireless networks in a satisfactory manner. The integration of MIMO transmission techniques to GFDM has been shown for space-time coding (STC) [1] and spatial multiplexing [9]. Furthermore, in order to combat with inter-antenna interference (IAI) and reduce the receiver complexity, the application of the SM-GFDM system has been considered in [10], where a poor error performance has been obtained due to the use of a suboptimal receiver. In addition, the combination of the IM technique [11] with GFDM has been investigated in [12], where a throughput loss was obtained due to the unused subcarriers. As a result, the existing studies on SM-GFDM and GFDM-IM are not satisfactory to improve the spectral efficiency as well as the error performance at the same time.

In this study, a novel MIMO-GFDM system, which combines GFDM with SFIM, is proposed. In order to enhance the error performance in a spectrum-efficient manner while preserving the advantages of the SM, combination of dual mode IM scheme with SM-GFDM is considered. Besides, an enhanced MIMO-GFDM receiver based on joint MIMO detection and GFDM demodulation is presented. We show that the GFDM-SFIM system achieves significantly better error performance than SM-GFDM system.

The remaining sections are organized as follows. Section II presents the GFDM-SFIM system model. Section III investigates the bit error ratio (BER) performance of the GFDM-SFIM system with respect to the SM-GFDM system and OFDM-SFIM system for Rayleigh multipath fading channels. Finally, Section IV concludes the paper.

978-1-5090-5049-9/17/$31.00 ©2017 IEEE

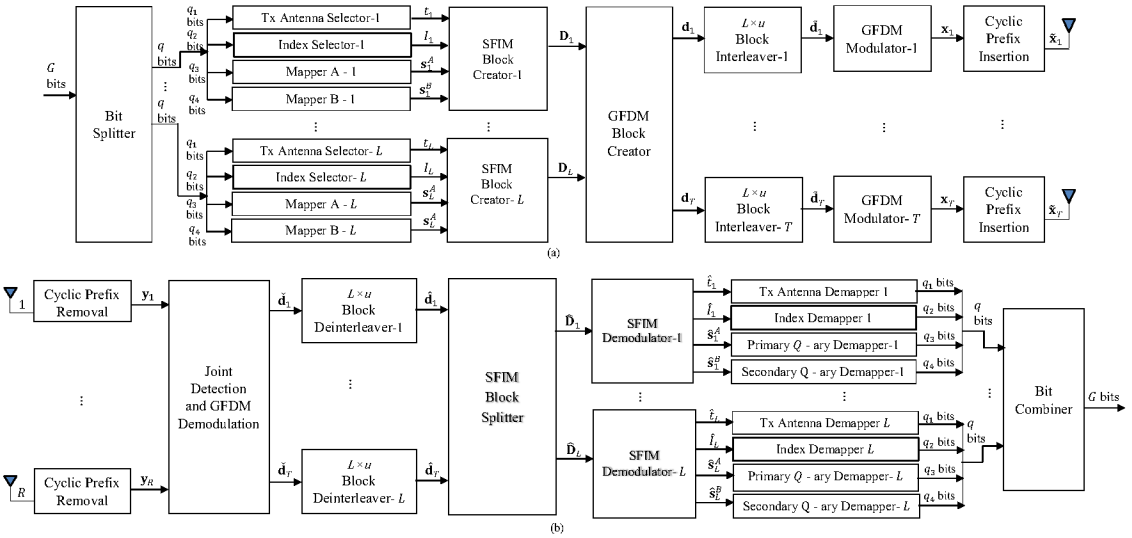


Fig. 1. Block diagram of GFDM-SFIM, (a) GFDM-SFIM transmitter, (b) GFDM-SFIM receiver.

## II. System Model

### A. GFDM-SFIM Transmitter

In this study, a MIMO-GFDM system with $T$ transmit and $R$ receive antennas is considered. The block diagram of the proposed GFDM-SFIM transmitter is given in Fig. 1(a). Bit splitter partitions $G$ incoming bits into $L$ groups each containing $q$ bits, i.e., $q = G/L$. Then, each group of $q$ bits is mapped to a subcarrier group with $u$ elements. In this mapping operation, antenna and subcarrier indices as well as $Q$-ary quadrature amplitude modulation ($Q$-QAM) constellations are used. The first $q_1 = \log_2(T)$ bits of the $q$-bit sequence are used to select the transmitting antenna index of the subcarrier group. After that, the first $q_2$ bits of the remaining bits are fed into index selector to partition the indices of each subcarrier group into two index subgroups, denoted as

$$I_l^A = \left\{ i_{l,1}^A, i_{l,2}^A, \ldots, i_{l,v}^A \right\}, \tag{1}$$

$$I_l^B = \left\{ i_{l,1}^B, i_{l,2}^B, \ldots, i_{l,u-v}^B \right\}, \tag{2}$$

where $i_{l,\gamma}^A \in \{1, \ldots, u\}$, for $\gamma = 1, \ldots, v$, $i_{l,\gamma}^B \in \{1, \ldots, u\}$, for $\gamma = 1, \ldots, u - v$ and $l \in \{1, \ldots, L\}$. Here, $I_l^A$ is determined first to modulate $v$ subcarriers by a selection rule and the remaining $u - v$ subcarriers constitute the $I_l^B$, hence, index selector has to define $I_l^A$ only. Since $I_l^A$ has $2^{q_2}$ possible realizations, only $c$ out of $C(u, v)$ possible combinations are used. Therefore, $q_2$ can be defined as

$$q_2 = \lfloor \log_2 \left( C(u, v) \right) \rfloor, \tag{3}$$

where $\lfloor \cdot \rfloor$ does the integer floor operation. Then, the remaining $q_3$ and $q_4$ bits are fed into mappers A and B to modulate the subcarriers selected by $I_l^A$ and $I_l^B$, respectively. Mapper A uses constellation set of $\mathcal{S}^A$, which has $Q_A$ elements, to modulate $v$ subcarriers and Mapper B uses constellation set of $\mathcal{S}^B$, which has $Q_B$ elements, to modulate $u - v$ subcarriers. Therefore, $q_3$ and $q_4$ can be defined as

$$q_3 = v \log_2(Q_A), \tag{4}$$

$$q_4 = (u - v) \log_2(Q_B). \tag{5}$$

At this point, in order to reliably detect the index subgroups at the receiver, the constellations used by the mappers A and B have to be disjoint sets, i.e., $\mathcal{S}^A \cap \mathcal{S}^B = \varnothing$. As a result, the vector of the modulated symbols mapped by Mapper A for the index subgroup $I_l^A$, which carries $q_3$ bits, and the vector of the modulated symbols mapped by Mapper B for the index subgroup $I_l^B$, which carries $q_4$ bits, can be expressed by

$$\mathbf{s}_l^A = \left[ s_l^A(1), s_l^A(2), \ldots, s_l^A(v) \right]^T, \tag{6}$$

$$\mathbf{s}_l^B = \left[ s_l^B(1), s_l^B(2), \ldots, s_l^B(u - v) \right]^T, \tag{7}$$

where $s_l^A(\gamma) \in \mathcal{S}^A$, $\gamma = 1, \ldots, v$, $s_l^B(\gamma) \in \mathcal{S}^B$, $\gamma = 1, \ldots, u - v$, respectively. Then, SFIM block creator combines $\mathbf{s}_l^A$ and $\mathbf{s}_l^B$ and creates the vector of the modulated symbols for the subcarrier group $(t_l, l)$, which will be assigned to the transmit antenna $t_l$ as

$$\mathbf{s}_{t_l,l} = \left[ s_{t_l,l}(1), s_{t_l,l}(2), \ldots, s_{t_l,l}(u) \right]^T, \tag{8}$$

where $s_{t_l,l}(\gamma) \in \{\mathcal{S}_A, \mathcal{S}_B\}$, for $t_l \in \{1, \ldots, T\}$ and $\gamma = 1, \ldots, u$. Afterwards, SFIM block creator sets the subcarriers of the inactive antennas to zero and arranges the transmit symbols for block $l$ in a $T \times u$ matrix $\mathbf{D}_l$, where $t_l$th row of $\mathbf{D}_l$ is $\mathbf{s}_{t_l,l}$. GFDM block creator combines the SFIM blocks in a $T \times N$ matrix $\mathbf{D} = [\mathbf{D}_1, \mathbf{D}_2, \ldots, \mathbf{D}_L]$, where $N = uL$ is the total number of samples in a GFDM block. As a result, the GFDM symbol for the transmit antenna $t$, which is $t$th row vector of $\mathbf{D}$, can be expressed by

$$\mathbf{d}_t = \left[ d_{t,0,0}, \ldots, d_{t,K-1,0}, d_{t,0,1}, \ldots, d_{t,K-1,M-1} \right], \tag{9}$$

where $d_{t,k,m}$ is the data symbol of $m$th timeslot on $k$th subcarrier belonging to $t$th antenna, $K$ and $M$ stand for the number of subcarriers and subsymbols, respectively. In [8] and [12], a block interleaver is used to render the channel memoryless; therefore, $L \times u$ block interleaving is applied to $\mathbf{d}_t$ and the interleaved data vector $\tilde{\mathbf{d}}_t$ is obtained. After

TABLE I
COMPUTATIONAL COMPLEXITY

| Process | ZF-SDD based SM-GFDM Receiver | MMSE-JDD based GFDM-SFIM Receiver |
|---|---|---|
| Detection | $2N^2R + 2NT^2R + NT^3 + NTR + 2N^2T$ | - |
| GFDM Demodulation | $N^2T$ | $2N^3T^2R + N^3T^3 + N_{Ch}N^2RT + N^2RT$ |
| Decision | $NT + NQ$ | $(N/u)ucQ_a^vQ_b^{u-v}$ |
| Complexity Order | $\sim \mathcal{O}(N^2(3T + 2R))$ | $\sim \mathcal{O}(N^3(2T^2R + T^3) + NQ_a^vQ_b^{u-v})$ |

block interleaving, $\widetilde{\mathbf{d}}_t$ is modulated using a GFDM modulator and the overall GFDM transmit signal $x_t(n)$ of $t$th transmit antenna is given by

$$x_t(n) = \sum_{k=0}^{K-1}\sum_{m=0}^{M-1} \widetilde{d}_{t,k,m} g\left((n - mK)_{\text{mod}N}\right) \exp\left(j2\pi\frac{kn}{K}\right), \tag{10}$$

where $n \in \{0, \ldots, N-1\}$ denotes the sampling index and $g(n)$ is the transmit filter circularly shifted to the $m$th timeslot and modulated to the $k$th subcarrier. (10) can be rewritten as $\mathbf{x}_t = \mathbf{A}\widetilde{\mathbf{d}}_t$, where $\mathbf{A}$ is an $N \times N$ transmitter matrix [1]. The last step at the transmitter side is the addition of a CP with length $N_{\text{CP}}$ in order to make the convolution with the channel circular.

### B. GFDM-SFIM Receiver

The block diagram of the proposed GFDM-SFIM receiver is given in Fig. 1(b). After the removal of CP, assuming that CP is longer than the tap length of the channel ($N_{\text{Ch}}$) and perfect synchronization is ensured, the overall received signal can be expressed as

$$\begin{bmatrix}\mathbf{y}_1\\ \vdots \\ \mathbf{y}_R\end{bmatrix} = \begin{bmatrix}\mathbf{H}_{1,1}\mathbf{A} & \cdots & \mathbf{H}_{1,T}\mathbf{A}\\ \vdots & \ddots & \vdots \\ \mathbf{H}_{R,1}\mathbf{A} & \cdots & \mathbf{H}_{R,T}\mathbf{A}\end{bmatrix}\begin{bmatrix}\widetilde{\mathbf{d}}_1\\ \vdots \\ \widetilde{\mathbf{d}}_T\end{bmatrix} + \mathbf{w}, \tag{11}$$

where $\mathbf{y}_r$ is the vector of received signals at the $r$th receive antenna, $\mathbf{H}_{r,t}$, for $t = 1, \ldots, T$, $r = 1, \ldots, R$, is the circular convolution matrix constructed from the channel impulse response coefficients between the $t$th transmit antenna and the $r$th receive antenna given by $\mathbf{h}_{r,t} = [h_{t,r,1}, \ldots, h_{t,r,N_{\text{Ch}}}]^{\text{T}}$, where $h_{t,r,n}$ follows $\mathcal{CN}(0,1)$ distribution, $\mathbf{w}$ is an $NT \times 1$ vector of additive white Gaussian noise (AWGN) samples with elements distributed as $\mathcal{CN}(0, \sigma_w^2)$. (11) can be rewritten in a more compact form as

$$\mathbf{y} = \widetilde{\mathbf{H}}\widetilde{\mathbf{d}} + \mathbf{w}, \tag{12}$$

where the dimensions of $\mathbf{y}$, $\widetilde{\mathbf{H}}$ and $\widetilde{\mathbf{d}}$ are $NR \times 1$, $NR \times NT$ and $NT \times 1$, respectively. For MIMO-OFDM case, joint MIMO detection and demodulation can be performed at the subcarrier level due to orthogonality in the frequency domain. In GFDM, the inherent intercarrier interference (ICI) prevents the frequency domain decoupling of GFDM subcarriers for both single-input single-output (SISO) and MIMO transmission schemes. Therefore, in order to realize joint MIMO detection and GFDM demodulation, all subcarriers belonging to all GFDM subsymbols must be processed together. Thanks to system model of (12), unlike SM-GFDM receiver in [10], which uses zero-forcing (ZF) detector in the frequency domain, thus, handles MIMO detection and GFDM demodulation separately, GFDM modulation and MIMO channel can be linearly modeled. As a result, joint MIMO detection and GFDM demodulation (JDD) through minimum mean squared error (MMSE) filtering can be performed by

$$\breve{\mathbf{D}} = \left(\widetilde{\mathbf{H}}^{\text{H}}\widetilde{\mathbf{H}} + \sigma_w^2\mathbf{I}\right)^{-1}\widetilde{\mathbf{H}}^{\text{H}}\mathbf{y}, \tag{13}$$

where $t_l$th row of $\breve{\mathbf{D}}$ is $\breve{\mathbf{d}}_t$, which is the estimation of the output of the $t_l$th block interleaver. This method is named as MMSE-JDD. Note that, MMSE-JDD is also applicable for SM and space shift keying (SSK) based GFDM systems. Afterwards, $L \times u$ block deinterleaving is applied to $\breve{\mathbf{d}}_t$ and $\widehat{\mathbf{d}}_t$ is obtained. SFIM block splitter partitions $\widehat{\mathbf{d}}_t$ into L groups with length $u$ and arranges these groups in a $T \times u$ matrix given by

$$\widehat{\mathbf{D}}_l = \begin{bmatrix}\hat{\mathbf{s}}_{1,l}\\ \vdots \\ \hat{\mathbf{s}}_{T,l}\end{bmatrix} = \begin{bmatrix}\widehat{\mathbf{d}}_1((l-1)u+1:lu)\\ \vdots \\ \widehat{\mathbf{d}}_T((l-1)u+1:lu)\end{bmatrix}. \tag{14}$$

Then, SFIM makes a joint decision on the active transmit antenna index, subcarrier index subgroup as well as constellation symbols considering all possible realizations of $\mathbf{D}_l$ by minimizing the following metric:

$$\left\{\hat{t}_l, \hat{I}_l^A, \hat{\mathbf{s}}_l^A, \hat{\mathbf{s}}_l^B\right\} = \underset{t, I^A, \mathcal{S}^A, \mathcal{S}^B}{\text{argmin}} \left\|\widehat{\mathbf{D}}_l - \mathbf{D}_l\right\|_F^2. \tag{15}$$

Finally, the original information bits are retrieved by the subsequent blocks.

### C. Computational Complexity

Computational complexities of the SM-GFDM receiver, which uses ZF-based separate MIMO detection and demodulation (ZF-SDD) given in [10] and the GFDM-SFIM receiver are analyzed in terms of total number of complex multiplications (CMs) and presented in Table I. According to Table I, it is observed that the complexity of the GFDM-SFIM receiver increases with the increasing value of the number of transmit and receive antennas as well as the number of subcarriers and subsymbols. As mentioned before, MMSE-JDD is also applicable for SM-GFDM system. Since only the decision part of the GFDM-SFIM system causes a negligible amount of complexity increase, the computational complexity of the

TABLE II
SIMULATION PARAMETERS

| Description | Parameter | Value |
|---|---|---|
| Number of subcarriers | $K$ | 128 |
| Number of subsymbols | $M$ | 5 |
| Pulse shaping filter | $g$ | RRC |
| Length of cyclic prefix | $N_{\text{CP}}$ | 32 |
| Exponent of power delay profile | $\phi$ | 0.1 |
| Number of channel taps | $N_{\text{Ch}}$ | 10 |

TABLE III
A LOOK-UP TABLE EXAMPLE FOR $u = 4, v = 2$

| *Bits* | *Indices* | *subgroups* |
|---|---|---|
| [0 0] | $\{1, 2\}$ | $\left[s_l^A(1)\ s_l^A(2)\ s_l^B(1)\ s_l^B(2)\right]^T$ |
| [0 1] | $\{2, 3\}$ | $\left[s_l^B(1)\ s_l^A(1)\ s_l^A(2)\ s_l^B(2)\right]^T$ |
| [1 0] | $\{3, 4\}$ | $\left[s_l^B(1)\ s_l^B(2)\ s_l^A(1)\ s_l^A(2)\right]^T$ |
| [1 1] | $\{1, 4\}$ | $\left[s_l^A(1)\ s_l^B(1)\ s_l^B(2)\ s_l^A(2)\right]^T$ |

GFDM-SFIM system and the MMSE-JDD based SM-GFDM system is approximately same.

### D. Spectral Efficiency

In GFDM-SFIM, active transmit antenna selection for each subcarrier group instead of each subcarrier reduces the spectral efficiency with respect to classical SM scheme. In order to compensate the spectral efficiency loss, either the modulation order or the transmit antenna size can be increased. On the other hand, GFDM uses a single CP for the entire symbol block composed of $K$ subcarriers with $M$ timeslots. Thus, spectral efficiency gain of the GFDM-SFIM system over OFDM-SFIM with the same system parameters becomes

$$\begin{aligned}\rho &= 100\frac{\frac{\frac{KM}{u}\log_2\left(TcQ_A^uQ_B^{(u-v)}\right)}{T(KM+N_{\text{CP}})} - \frac{\frac{K}{u}\log_2\left(TcQ_A^uQ_B^{(u-v)}\right)}{T(K+N_{\text{CP}})}}{\frac{\frac{K}{u}\log_2\left(TcQ_A^uQ_B^{(u-v)}\right)}{T(K+N_{\text{CP}})}} \\ &= 100\frac{N_{\text{CP}}(M-1)}{KM+N_{\text{CP}}}\%.\end{aligned} \tag{16}$$

## III. RESULTS AND DISCUSSION

In this section, the BER performance of the proposed GFDM-SFIM scheme, the SM-GFDM scheme and the OFDM-SFIM scheme are compared by computer simulations for Rayleigh multipath fading channels with the system parameters given in Table II. In order to determine the subcarrier index subgroups, a look-up table given in Table III is used. For binary phase shift keying (BPSK) transmission, the constellations $\mathcal{S}^A = \{-1, +1\}$ and $\mathcal{S}^B = \{-j, +j\}$ are used by Mapper A and Mapper B, respectively. For 4-QAM transmission, the constellations employed in [6] are used. These constellations are defined as $\mathcal{S}^A = \{-1-j, 1-j, 1+j, -1+j\}$ and $\mathcal{S}^B = \left\{1+\sqrt{3}, (1+\sqrt{3})j, -1-\sqrt{3}, -(1+\sqrt{3})j\right\}$ for Mapper A and Mapper B, respectively.

Fig. 2 compares the BER performance of the proposed GFDM-SFIM scheme to the ZF-SDD based SM-GFDM scheme given in [10] for a $2 \times 2$ MIMO configuration with roll-off factor ($\alpha$) of 0.1 and 0.5. From Fig. 2(a), for BPSK transmission at a BER value of $10^{-4}$, it is observed that the proposed GFDM-SFIM scheme achieves approximately 15 dB better BER performance than the ZF-SDD based SM-GFDM scheme at the cost of a slightly decreased spectral efficiency. From Fig. 2(b), it is observed that the BER performance improvement of the GFDM-SFIM scheme is 7 dB for 4-QAM transmission. This significant performance improvement arises from the MMSE-based joint MIMO detection and GFDM demodulation performed by the GFDM-SFIM receiver and the improved Euclidean distance spectrum due to IM. Note that increasing the modulation order of the GFDM-SFIM scheme decreases the BER improvement and increasing the roll-off factor slightly degrades the performance. On the other hand, according to Tables I and II, the computational complexity of the GFDM-SFIM receiver and the ZF-SDD based SM-GFDM receiver, required to implement the configurations given in Fig. 2, are on the order of $\sim \mathcal{O}(4.2 \times 10^9)$ and $\sim \mathcal{O}(4.1 \times 10^6)$, respectively. As a result, the GFDM-SFIM system can provide an interesting trade-off between the complexity and the BER performance.

Fig. 3 shows the BER performance of the proposed GFDM-SFIM scheme, OFDM-SFIM scheme and the ZF-SDD based and the MMSE-JDD based SM-GFDM schemes for $4 \times 4$ MIMO configuration. For GFDM schemes, a roll-off factor of 0.1 is used and for OFDM scheme, $M$ is equal to 1. From Figs. 2(b) and 3, it is observed that increasing the number of antennas enhances the BER performance of the GFDM-SFIM scheme. The reason behind this improvement is the increased diversity order due to MMSE detector used by the GFDM-SFIM receiver. From Fig. 3, thanks to this increased diversity order, joint MIMO detection and GFDM demodulation and the improved Euclidean distance spectrum due to IM, it is observed that the GFDM-SFIM scheme with 4-QAM transmission achieves approximately 14 dB better BER performance than the ZF-SDD based SM-GFDM scheme with BPSK transmission at the same spectral efficiency. It is also observed that the MMSE-JDD based SM-GFDM scheme achieves approximately 8 dB better BER performance than the ZF-SDD based SM-GFDM scheme and the GFDM-SFIM scheme still achives 6 dB better BER performance than the MMSE-JDD based SM-GFDM scheme at the same computational complexity. On the other hand, it is observed that the BER performance of the GFDM-SFIM scheme and the MMSE-JDD based OFDM-SFIM scheme is approximately same whereas the GFDM-SFIM scheme provides 19% spectral efficiency gain over the OFDM-SFIM schemes. Note that in GFDM, pulse shaping with root-raised cosine (RRC) filter reduces OOB emission significantly and nonorthogonal subcarriers allow loose time and frequency synchronization.

Fig. 4 compares the BER performance of the GFDM-SFIM scheme for a $4 \times 4$ MIMO configuration to the ZF-SDD based SM-GFDM scheme for a $2 \times 2$ MIMO configuration with a roll-off factor of 0.1. From Fig. 4, at a BER value of $10^{-4}$, it is observed that the GFDM-SFIM scheme achieves

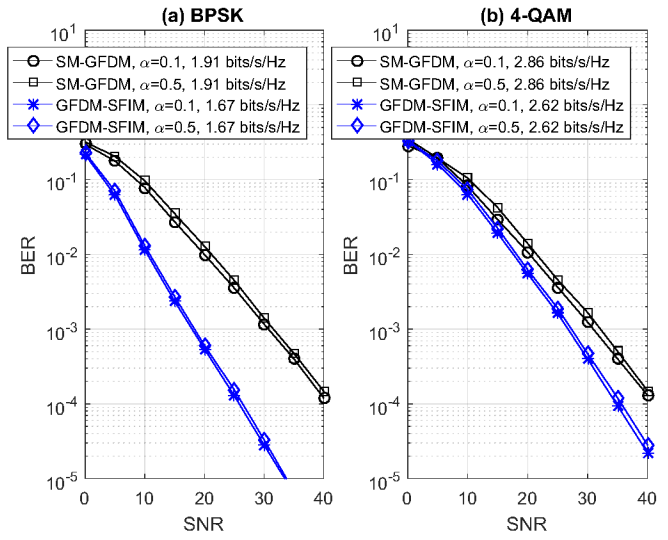


Fig. 2. BER performance of the GFDM-SFIM and the ZF-SDD based SM-GFDM for a 2 × 2 MIMO configuration with (a) BPSK (b) 4-QAM transmissions.

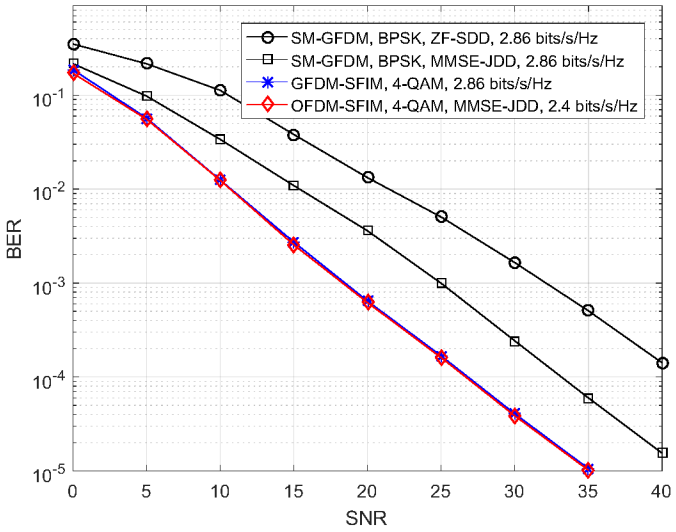


Fig. 3. BER performance of the GFDM-SFIM and SM-GFDM with roll-off factor of 0.1 and OFDM-SFIM systems for a 4 × 4 MIMO configuration.

approximately 22 dB and 12 dB better BER performance than the ZF-SDD based SM-GFDM scheme at the same spectral efficiency for BPSK and 4-QAM transmissions, respectively.

## IV. Conclusion

In this paper, a novel MIMO-GFDM system, which combines GFDM with SFIM, has been proposed. The system model of the proposed GFDM-SFIM scheme has been presented and its BER performance has been compared to SM-GFDM and OFDM-SFIM systems under Rayleigh multipath fading channels. It has been shown that SFIM is applicable to MIMO-GFDM application and provides significant BER improvements compared to SM-GFDM scheme and spectral efficiency compared to OFDM-SFIM scheme. Besides, IAI in spatial multiplexing transmission scheme is avoided and only inherent GFDM interferences, such as ICI and inter

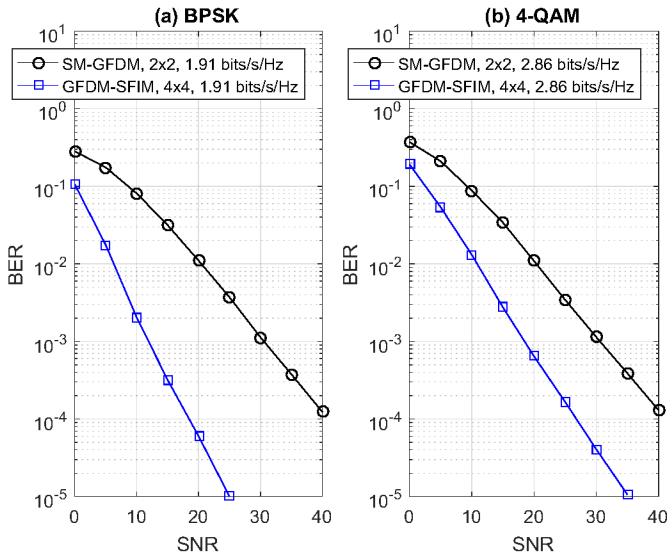


Fig. 4. BER performance of the GFDM-SFIM for a 2×2 MIMO configuration and the ZF-SDD based SM-GFDM for a 4 × 4 MIMO configuration with (a) BPSK (b) 4-QAM transmissions using roll-off factor of 0.1.

subsymbol interference effect the system performance. As a future study, we will investigate the optimum or near-optimum detection methods, which combine MIMO detection, GFDM demodulation and SFIM demodulation with reduced complexity.

## References


[1] N. Michailow, M. Matthe, I. Gaspar, A. Caldevilla, L. Mendes, A. Festag, and G. Fettweis, "Generalized frequency division multiplexing for 5th generation cellular networks," *IEEE Trans. Commun.*, vol. 62, no. 9, pp. 3045–3061, Sep. 2014.

[2] R. Mesleh *et. al.*, "Spatial modulation," *IEEE Trans. Veh. Technol.*, vol. 57, no. 4, pp. 2228–2241, Jul. 2008.

[3] E. Basar, Ü. Aygölü, E. Panayırcı, and H. V. Poor, "Orthogonal frequency division multiplexing with index modulation," *IEEE Trans. Signal Process.*, vol. 61, no. 22, pp. 5536–5549, Nov. 2013.

[4] R. Abu-alhiga and H. Haas, "Subcarrier-index modulation OFDM," in *IEEE Int. Sym. Personal, Indoor and Mobile Radio Commun.*, Tokyo, Japan, Sep. 2009, pp. 177–181.

[5] D. Tsonev, S. Sinanovic, and H. Haas, "Enhanced subcarrier index modulation (SIM) OFDM," in *IEEE GLOBECOM Workshops*, Dec. 2011, pp. 728–732.

[6] T. Mao, Z. Wang, Q. Wang, S. Chen, and L. Hanzo, "Dual-mode index modulation aided OFDM," *IEEE Access*, vol. PP, no. 99, pp. 1–1, 2016.

[7] T. Datta, H. S. Eshwaraiah, and A. Chockalingam, "Generalized space-and-frequency index modulation," *IEEE Trans. Veh. Technol.*, vol. 65, no. 7, pp. 4911–4924, 2016.

[8] E. Basar, "On multiple-input multiple-output OFDM with index modulation for next generation wireless networks," *IEEE Trans. Signal Process.*, vol. 64, no. 15, pp. 3868–3878, Aug. 2016.

[9] M. Matthe, I. Gaspar, D. Zhang, and G. Fettweis, "Near-ML detection for MIMO-GFDM," in *Proc. 82nd IEEE Veh. Technol. Conf. Fall*, Boston, USA, Sep. 2015.

[10] E. Ozturk, E. Basar, and H. Cirpan, "Spatial modulation GFDM: A low complexity MIMO-GFDM system for 5G wireless networks," in *Proc. 4th IEEE Int. Black Sea Conf. Commun. Networking*, Varna, Bulgaria, Jun. 2016.

[11] E. Basar, "Index modulation techniques for 5G wireless networks," *IEEE Commun. Mag.*, vol. 54, no. 7, pp. 168–175, Jul. 2016.

[12] E. Ozturk, E. Basar, and H. Cirpan, "Generalized frequency division multiplexing with index modulation," in *Proc. IEEE GLOBECOM Workshops*, Washington DC, USA, Dec. 2016.